Supporting Information for: Order-by-disorder in the antiferromagnetic Ising model on an elastic triangular lattice

Yair Shokef*, Anton Souslov† and Tom C. Lubensky†
*Department of Materials and Interfaces, Weizmann Institute of Science, Rehovot 76100, Israel
†Department of Physics and Astronomy, University of Pennsylvania, Philadelphia, PA 19104, USA

This document provides further details on the analytical calculations behind the results presented in the main text of the paper. We begin with a full description of the ground state in Sec. I, and then devote the remainder of the document to the low-temperature expansion, the results of which are summarized in Fig. 6 in the paper. We performed this low-temperature expansion in two complementary techniques, and verified that they produce exactly the same results when exact comparison was possible. As will be seen below, we employed both approaches since different information and insights on the system may be gained from each one of them.

The 'logical' approach, described in Sec. II treats the excitations from the point of view of small oscillations of a mechanical system with a large (but finite) number of particles. Due to the periodicity of the ground states that we analyze, the normal modes are described by plane waves. However, in this logical approach, we write the plane waves in terms of the logical indices of the particles in the system rather than in terms of their physical positions, which is the standard way of describing phonons in a lattice. Our use of the logical wavevectors causes the reciprocal space to be invariant with respect to the deformations of the lattice and to be fixed for all spin configurations within the ground state. This enables us to easily compare the dispersion relations of different ground-state configurations and to analyze the differences in their contribution to the free energy. However, these calculations become increasingly tedious with increasing unit-cell size, and we limit ourselves to the two simplest cases of straight stripes and bent stripes. The comparison between these two extreme cases in the logical approach enables us to understand the origins for the non-monotonic behavior of the free energy difference between the two, shown in Fig. 6D in the paper.

In Sec. III we give the standard 'physical' approach which describes the normal modes by plane waves in terms of the physical position of the particles. For an undeformed lattice, the logical and physical approaches are equivalent, but since we are dealing with deformed lattices, they differ. We first give the derivation for straight stripes and for bent stripes and verify that the dispersion relations and the free energy coefficients coincide with the results of the logical approach. Then, we use the modular structure of the dynamical matrix in the physical approach to construct a scheme for calculating the free energy for ground state configurations with larger unit cells. The results of these calculations are presented in Fig. 6A-C in the paper and are given in more detail here.

I. GROUND STATE

In the ground state, each triangular plaquette has two satisfied bonds ($\sigma_i\sigma_j=-1$) of length sa and one frustrated bond ($\sigma_i\sigma_j=1$) of length fa. Requiring that the area of this isosceles triangle is equal to that of an equilateral triangle of sides a, leads to $f(\beta)=3^{1/4}(\tan\frac{\beta}{2})^{1/2}$, $s(\beta)=3^{1/4}\left(2\sin\beta\right)^{-1/2}$, where β is the head angle of the isosceles triangle. Upon substitution in Eq. (1) we see that the energy of each such triangle is given by

$$E=J[-2(1-\epsilon a(s-1))+(1-\epsilon a(f-1))]+\frac{Ka^2}{2}[2(s-1)^2+(f-1)^2] \tag{S1}$$

Minimizing this with respect to β leads to

$$\frac{dE}{d\beta}=J\epsilon a(2s'-f')+Ka^2[2(s-1)s'+(f-1)f']=0 \tag{S2}$$

Which is equivalent to Eq. (2). β clearly depends on the dimensionless ratio $b\equiv\frac{J\epsilon}{Ka}$, but we cannot obtain an explicit solution for $\beta(b)$. Instead, we obtain

$$b(\beta)=\frac{2(s-1)s'+(f-1)f'}{f'-2s'}=\frac{1-2\sin\left(\frac{\beta}{2}\right)}{1-\sin\left(\frac{\beta}{2}\right)}\left[\frac{1+\sin\left(\frac{\beta}{2}\right)}{1+2\sin\left(\frac{\beta}{2}\right)}-\left(2\sin\beta\right)^{-1/2}\right] \tag{S3}$$

which we plot in Fig. 1B.

II. DISPERSION RELATIONS IN TERMS OF LOGICAL WAVEVECTORS

In the following we will consider various ground-state configurations. For each one, the particle positions at their mechanical equilibrium are given by $\{x_i, y_i\}$, and we will deal with small displacements $\{u_i, v_i\}$ about these positions. The distance between particles i and j is given by

$$dr^2 = (dx + du)^2 + (dy + dv)^2 = dr_0^2 + 2(dxdu + dydv) + du^2 + dv^2 \tag{S4}$$

where $dx = x_i - x_j$, $dy = y_i - y_j$, $du = u_i - u_j$, $dv = v_i - v_j$, and $dr_0 = (dx^2 + dy^2)^{1/2}$ is the equilibrium separation between the particles. Since we will expand around mechanical equilibria, we may ignore the terms linear in du or dv and write

$$dr^2 = dr_0^2 + du^2 + dv^2. \tag{S5}$$

Some terms in the harmonic expansion of the system's energy contain also terms linear in dr. We therefore take the square root of Eq. (S4) and expand to harmonic order to obtain:

$$dr = dr_0 + \frac{du^2}{2dr_0}\left(1 - \frac{dx^2}{dr_0^2}\right) + \frac{dv^2}{2dr_0}\left(1 - \frac{dy^2}{dr_0^2}\right) - \frac{dxdydudv}{dr_0^3}. \tag{S6}$$

A. Straight Stripes

We begin with the simplest ground-state configuration of straight stripes, for which the unit cell consists of a single particle. Figure S1 shows a particle and its neighbors. We label the particle with 0 and its neighbors with $1-6$. Note that x and y are real variables denoting the physical position of each particle in the two-dimensional plane, whereas m and n are integers used to label the index of the particle in the triangular network. Also note that in the straight-stripe ground-state, although in terms of the Ising states the unit-cell consists of two particles, for the elastic considerations the up and down states behave equivalently and we may use a single-particle unit-cell.

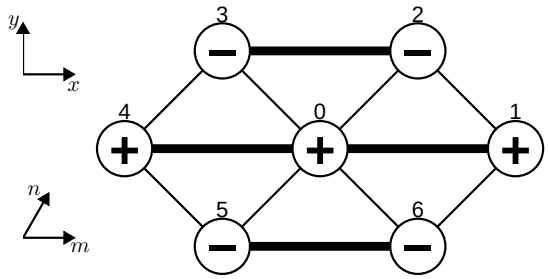

FIG. S1: Neighboring particles of each particle in the lattice in the straight-stripes configuration. Thick lines correspond to the frustrated bonds.

The indices and positions at mechanical equilibrium of the central particle and its six neighbors are given in Table S1. We have used the dimensionless lengths f and s of the frustrated and satisfied bonds, and $h = \sqrt{s^2 - f^2/4}$ which is the dimensionless height of each isosceles triangle.

	i	dx/a	dy/a	dr/a	$\sigma_i\sigma_j$
0	(m, n)	0	0	0	
1	$(m+1, n)$	f	0	f	1
2	$(m, n+1)$	$f/2$	h	s	-1
3	$(m-1, n+1)$	$-f/2$	h	s	-1
4	$(m-1, n)$	$-f$	0	f	1
5	$(m, n-1)$	$-f/2$	$-h$	s	-1
6	$(m+1, n-1)$	$f/2$	$-h$	s	-1

TABLE S1: Indices and positions of the neighbors in a straight-stripe configuration.

We may now write the total energy of the system as

$$\mathcal{H} = \sum_{m,n} \sum_{\ell=1}^{3} \left\{ \left[1 - \epsilon \left(dr_\ell - a\right)\right] J\sigma_0\sigma_l + \frac{K}{2}\left(dr_\ell - a\right)^2 \right\}. \tag{S7}$$

Instead of the sum over nearest-neighbor pairs $< i, j >$ in Eq. (1) in the main text, here we sum over all particles (m, n) and additionally sum over three of the six neighbors each particle has. In this way each bond in the system is counted once. In Eq. (S7) we have suppressed the indices m, n from dr and σ and instead denote the neighbors by $1 \leq \ell \leq 3$. By substituting the spin values of all neighbors in a straight-stripe configuration according to Table S1 we obtain,

$$\mathcal{H} = \sum_{m,n} \Big[- J\epsilon \left(dr_1 - dr_2 - dr_3\right) - Ka \left(dr_1 + dr_2 + dr_3\right) + \frac{K}{2}\left(dr_1^2 + dr_2^2 + dr_3^2\right) \Big], \tag{S8}$$

where here and in the following we supress additive constants without announcing. By inserting the positions of neighbors according to Table S1 and using Eqs. (S6) and (S5) we write,

$$\begin{aligned} \mathcal{H} = \frac{K}{2} \sum_{m,n} \Bigg\{ & \frac{-b-1}{f} dv_1^2 \;+\; \frac{b-1}{s} \left[\left(1 - \frac{f^2}{4s^2}\right)\left(du_2^2 + du_3^2\right) + \left(1 - \frac{h^2}{s^2}\right)\left(dv_2^2 + dv_3^2\right) + \frac{fh}{s^2}\left(-du_2 dv_2 + du_3 dv_3\right) \right] \\ & + \; \left(du_1^2 + du_2^2 + du_3^2 + dv_1^2 + dv_2^2 + dv_3^2\right) \Bigg\}. \end{aligned} \tag{S9}$$

Noting that $h^2 + f^2/4 = s^2$, this may be simplified to:

$$\begin{aligned} \mathcal{H} \;=\; & \frac{K}{2} \sum_{m,n} \Bigg[du_1^2 + \left(1 - \frac{b+1}{f}\right) dv_1^2 \\ & + \; \left(1 + \frac{h^2(b-1)}{s^3}\right)\left(du_2^2 + du_3^2\right) + \left(1 + \frac{f^2(b-1)}{4s^3}\right)\left(dv_2^2 + dv_3^2\right) + \frac{fh(b-1)}{s^3}\left(-du_2 dv_2 + du_3 dv_3\right) \Bigg]. \end{aligned} \tag{S10}$$

Noting that $du_\ell = u_\ell - u_0$ and $dv_\ell = v_\ell - v_0$ we obtain,

$$\begin{aligned} \mathcal{H} \;=\; & K \sum_{m,n} \Bigg[u_0^2 - u_0 u_1 + \left(1 - \frac{b+1}{f}\right)\left(v_0^2 - v_0 v_1\right) + \left(1 + \frac{h^2(b-1)}{s^3}\right)\left(2u_0^2 - u_0 u_2 - u_0 u_3\right) \\ & + \; \left(1 + \frac{f^2(b-1)}{4s^3}\right)\left(2v_0^2 - v_0 v_2 - v_0 v_3\right) + \frac{fh(b-1)}{2s^3}\left(u_0 v_2 + u_2 v_0 - u_0 v_3 - u_3 v_0\right) \Bigg]. \end{aligned} \tag{S11}$$

Recalling that

$$\begin{aligned} & u_0 = u_{m,n} \;\;,\;\; u_1 = u_{m+1,n} \;\;\;\;,\;\;\;\; u_2 = u_{m,n+1} \;\;,\;\; u_3 = u_{m-1,n+1} \\ & v_0 = v_{m,n} \;\;,\;\; v_1 = v_{m+1,n} \;\;\;\;,\;\;\;\; v_2 = v_{m,n+1} \;\;,\;\; v_3 = v_{m-1,n+1} \;\;\;\;, \end{aligned} \tag{S12}$$

the equations of motion are:

$$\begin{aligned} M\ddot{u}_{m,n} = -\frac{\partial \mathcal{H}}{\partial u_{m,n}} = \; & - \; K \Bigg[2u_{m,n} - u_{m+1,n} - u_{m-1,n} \\ & + \; \left(1 + \frac{h^2(b-1)}{s^3}\right)\left(4u_{m,n} - u_{m,n+1} - u_{m,n-1} - u_{m-1,n+1} - u_{m+1,n-1}\right) \\ & + \; \frac{fh(b-1)}{2s^3}\left(v_{m,n+1} + v_{m,n-1} - v_{m-1,n+1} - v_{m+1,n-1}\right) \Bigg] \\ M\ddot{v}_{m,n} = -\frac{\partial \mathcal{H}}{\partial v_{m,n}} = \; & - \; K \Bigg[\left(1 - \frac{b+1}{f}\right)\left(2v_{m,n} - v_{m+1,n} - v_{m-1,n}\right) \\ & + \; \left(1 + \frac{f^2(b-1)}{4s^3}\right)\left(4v_{m,n} - v_{m,n+1} - v_{m,n-1} - v_{m-1,n+1} - v_{m+1,n-1}\right) \\ & + \; \frac{fh(b-1)}{2s^3}\left(u_{m,n-1} + u_{m,n+1} - u_{m+1,n-1} - u_{m-1,n+1}\right) \Bigg]. \end{aligned} \tag{S13}$$

We now assume a solution of the form

$$u_{m,n} = Ue^{i(k_m m + k_n n - \omega_{\vec{k}} t)} \quad , \quad v_{m,n} = Ve^{i(k_m m + k_n n - \omega_{\vec{k}} t)} \tag{S14}$$

Note that since we perform a Fourier transform using the logical positions on the network, $1 \leq m, n \leq L$ (where $N = L^2$), rather than in terms of the physical position x, y in space, the allowed wavevectors are simply given by $k_m = 2\pi p/L$, $k_n = 2\pi q/L$, where $1 \leq p, q \leq L$, and summation over all these normal modes is much simpler than integrating over a geometrically more complicated Brillouin zone.

Substituting (S14) into Eq. (S13) transforms it to the following linear equation

$$\begin{pmatrix} A - \frac{M\omega^2}{K} & C \\ C & B - \frac{M\omega^2}{K} \end{pmatrix} \begin{pmatrix} U \\ V \end{pmatrix} = 0 \tag{S15}$$

where

$$\begin{aligned} A(\vec{k}) &\equiv 2(1 - \cos(k_m)) + 2\left(1 + \frac{h^2(b-1)}{s^3}\right)(2 - \cos(k_n) - \cos(k_m - k_n)) \\ B(\vec{k}) &\equiv 2\left(1 - \frac{b+1}{f}\right)(1 - \cos(k_m)) + 2\left(1 + \frac{f^2(b-1)}{4s^3}\right)(2 - \cos(k_n) - \cos(k_m - k_n)) \\ C(\vec{k}) &\equiv \frac{fh(b-1)}{s^3}(\cos(k_n) - \cos(k_m - k_n)) \end{aligned} \tag{S16}$$

Hence the eigen-frequencies of the system are

$$\frac{M\omega^2}{K} = \frac{1}{2}\left[A + B \pm \sqrt{(A-B)^2 + 4C^2}\right] \tag{S17}$$

Note that since we are interested in calculating $\mathcal{A} \equiv \frac{1}{N}\sum_k \log\left(\sqrt{\frac{M}{K}}\omega_k\right)$, and since frequencies appear in pairs, we can use the product of each pair of frequencies, which has the simple form

$$\left(\frac{M}{K}\right)^2 \omega_+^2 \omega_-^2 = AB - C^2. \tag{S18}$$

Thus,

$$\mathcal{A} = \frac{1}{2N}\sum_{\vec{k}} \log\left(AB - C^2\right). \tag{S19}$$

To write these dispersion relations in terms of the conventional physical wavevectors, we note that the position of particle (m, n) in the lattice is given by $x_{m,n} = afm + \frac{af}{2}n$, $y_{m,n} = ahn$. To equate the plane waves that we assumed above as a function of m and n with wavevector (k_m, k_n) to the conventional plane waves as a function of x and y with wavevector (q_x, q_y), we require that $q_x x + q_y y = k_m m + k_n$. For the straight stripes this leads to $k_m = afq_x$, $k_n = \frac{af}{2}q_x + ahq_y$. Upon substitution in Eqs. (S15), (S16), (S17), one obtains the dispersion relations as a function of (q_x, q_y) and it is straightforward to verify that the expressions are equivalent to those obtained in Sec. III B below where the entire derivation is in terms of the physical wavevectors.

B. Bent Stripes

The ground-state consisting of maximally zigzagging stripes has a unit cell of two particles. The positions of the 8 neighbors of the two particles in the unit cell are labeled in Fig. S2.

We use the fact that the lengths of the frustrated bonds are fa and of the satisfied bonds are sa and that the head angle of each isosceles triangle is β and the two small angles are $(\pi - \beta)/2$. It is then straightforward to obtain the positions of these 10 particles as given in Table S2, where we have set the position of particle 0 as the origin and chosen the x-direction to run along the line connecting particles 0 and 1. Particle 0 represents the particles with odd m, and particle 1 represents the particles with even m, hence we set for particle 0, $m = 2t - 1$, and for particle 1, $m = 2t$, where $1 \leq t \leq L/2$. The indices of the remaining neighbors are given in Table S2. From now on we will use

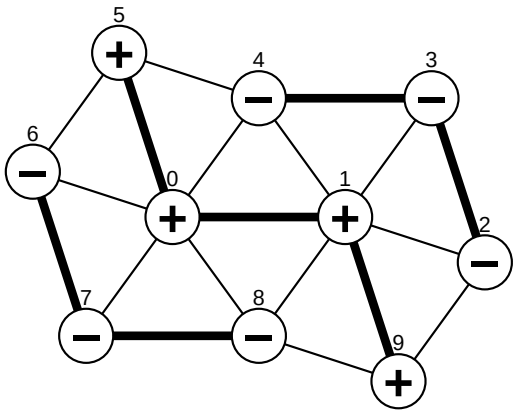

FIG. S2: Neighboring particles of the particles 0 and 1 in the unit cell of the maximally zigzagging stripe configuration. Thick lines correspond to the frustrated bonds.

ℓ	i	x/a	y/a
0	(m,n)	0	0
1	$(m+1,n)$	f	0
2	$(m+2,n)$	$f+s\sin(3\beta/2)$	$s\cos(3\beta/2)$
3	$(m+1,n+1)$	$f+s\sin(\beta/2)$	$s\cos(\beta/2)$
4	$(m,n+1)$	$s\sin(\beta/2)$	$s\cos(\beta/2)$
5	$(m-1,n+1)$	$-f\cos(\beta)$	$f\sin(\beta)$
6	$(m-1,n)$	$-s\sin(3\beta/2)$	$-s\cos(3\beta/2)$
7	$(m,n-1)$	$-s\sin(\beta/2)$	$-s\cos(\beta/2)$
8	$(m+1,n-1)$	$s\sin(\beta/2)$	$-s\cos(\beta/2)$
9	$(m+2,n-1)$	$f(1+\cos(\beta))$	$-f\sin(\beta)$

TABLE S2: Indices and positions of the neighbors in a maximally zigzagging stripe configuration.

the index t instead of m and denote the displacements of particles with odd m by $(u_{t,n}, v_{t,n})$ and of particles with even m by $(w_{t,n}, z_{t,n})$.

The distances between the particles 0 and 1 of the unit cell and all their neighbors are given in Table S3.

Using the values of $\sigma_i\sigma_j$ for all pairs (see Table S3), the energy of the system may be written as

$$\mathcal{H} = \sum_{t,n}\Big[\; - \; J\epsilon\,(dr_{10} - dr_{40} - dr_{41} - dr_{31} - dr_{21} + dr_{50}) - Ka\,(dr_{10} + dr_{40} + dr_{41} + dr_{31} + dr_{21} + dr_{50}) \\ + \; \frac{K}{2}\left(dr_{10}^2 + dr_{40}^2 + dr_{41}^2 + dr_{31}^2 + dr_{21}^2 + dr_{50}^2\right)\Big], \tag{S20}$$

where the summation is over all unit cells, that is over $1 \le t \le L/2$ and $1 \le n \le L$. We sum over 5 of the 10 bonds that the unit cell (i.e. particles 0 and 1) has with its neighboring unit cells such that when summing over unit cells each bond in the system will be counted once.

particles	dx/a	dy/a	dr/a	$\sigma_i\sigma_j$
1,0	f	0	f	1
4,0	$s\sin(\beta/2)$	$s\cos(\beta/2)$	s	-1
5,0	$-f\cos(\beta)$	$f\sin(\beta)$	f	1
6,0	$-s\sin(3\beta/2)$	$-s\cos(3\beta/2)$	s	-1
7,0	$-s\sin(\beta/2)$	$-s\cos(\beta/2)$	s	-1
8,0	$s\sin(\beta/2)$	$-s\cos(\beta/2)$	s	-1
2,1	$s\sin(3\beta/2)$	$s\cos(3\beta/2)$	s	-1
3,1	$s\sin(\beta/2)$	$s\cos(\beta/2)$	s	-1
4,1	$-s\sin(\beta/2)$	$s\cos(\beta/2)$	s	-1
8,1	$-s\sin(\beta/2)$	$-s\cos(\beta/2)$	s	-1
9,1	$f\cos(\beta)$	$-f\sin(\beta)$	f	1

TABLE S3: Distances between particles in a maximally zigzagging stripe configuration.

We now use Eqs. (S6) and (S5) and the values of dx and dy from Table S3 to obtain

$$\begin{aligned}\mathcal{H} &= \frac{K}{2}\sum_{t,n}\Bigg[du_{10}^2+\left(1-\frac{b+1}{f}\right)dv_{10}^2 \\ &+ \left(1-\frac{b+1}{f}\sin^2(\beta)\right)du_{50}^2+\left(1-\frac{b+1}{f}\cos^2(\beta)\right)dv_{50}^2-\frac{b+1}{f}\sin(2\beta)du_{50}dv_{50} \\ &+ \left(1+\frac{b-1}{s}\cos^2\left(\frac{\beta}{2}\right)\right)\left(du_{40}^2+du_{41}^2+du_{31}^2\right)+\left(1+\frac{b-1}{s}\cos^2\left(\frac{3\beta}{2}\right)\right)du_{21}^2 \\ &+ \left(1+\frac{b-1}{s}\sin^2\left(\frac{\beta}{2}\right)\right)\left(dv_{40}^2+dv_{41}^2+dv_{31}^2\right)+\left(1+\frac{b-1}{s}\sin^2\left(\frac{3\beta}{2}\right)\right)dv_{21}^2 \\ &+ \frac{b-1}{s}\sin(\beta)\left(-du_{40}dv_{40}+du_{41}dv_{41}-du_{31}dv_{31}\right)-\frac{b-1}{s}\sin(3\beta)du_{21}dv_{21}\Bigg]. \end{aligned} \tag{S21}$$

We now substitute

$$\begin{aligned} u_0 = u_{t,n}\ ,\ \ u_1 = w_{t,n}\ ,\ \ u_2 = u_{t+1,n}\ ,\ \ u_3 = w_{t,n+1}\ ,\ \ u_4 = u_{t,n+1}\ ,\ \ u_5 = w_{t-1,n+1} \\ v_0 = v_{t,n}\ ,\ \ v_1 = z_{t,n}\ ,\ \ v_2 = v_{t+1,n}\ ,\ \ v_3 = z_{t,n+1}\ ,\ \ v_4 = v_{t,n+1}\ ,\ \ v_5 = z_{t-1,n+1} \end{aligned} \tag{S22}$$

into Eq. (S21) and obtain (Note that it may be confusing that (u,v) are used for odd m but even ℓ and (w,z) are

used for even m but odd ℓ)

$$
\begin{aligned}
M\ddot{u}_{t,n} &= -\frac{\partial E}{\partial u_{t,n}} = -K\Big[-w_{t,n} + u_{t,n} + \left(1 - \frac{b+1}{f}\sin^2(\beta)\right)(-w_{t-1,n+1} + u_{t,n}) \\
&- \frac{b+1}{2f}\sin(2\beta)(-z_{t-1,n+1} + v_{t,n}) \\
&+ \left(1 + \frac{b-1}{s}\cos^2\left(\frac{\beta}{2}\right)\right)(3u_{t,n} - u_{t,n+1} - u_{t,n-1} - w_{t,n-1}) + \left(1 + \frac{b-1}{s}\cos^2\left(\frac{3\beta}{2}\right)\right)(u_{t,n} - w_{t-1,n}) \\
&+ \frac{b-1}{2s}\sin(\beta)(v_{t,n-1} + v_{t,n+1} - v_{t,n} - z_{t,n-1}) + \frac{b-1}{2s}\sin(3\beta)(-v_{t,n} + z_{t-1,n})\Big] \\
M\ddot{w}_{t,n} &= -\frac{\partial E}{\partial w_{t,n}} = -K\Big[w_{t,n} - u_{t,n} + \left(1 - \frac{b+1}{f}\sin^2(\beta)\right)(w_{t,n} - u_{t+1,n-1}) \\
&- \frac{b+1}{2f}\sin(2\beta)(z_{t,n} - v_{t+1,n-1}) \\
&+ \left(1 + \frac{b-1}{s}\cos^2\left(\frac{\beta}{2}\right)\right)(3w_{t,n} - u_{t,n+1} - w_{t,n+1} - w_{t,n-1}) + \left(1 + \frac{b-1}{s}\cos^2\left(\frac{3\beta}{2}\right)\right)(-u_{t+1,n} + w_{t,n}) \\
&+ \frac{b-1}{2s}\sin(\beta)(-v_{t,n+1} - z_{t,n} - z_{t,n-1} + z_{t,n+1}) + \frac{b-1}{2s}\sin(3\beta)(v_{t+1,n} - z_{t,n})\Big] \\
M\ddot{v}_{t,n} &= -\frac{\partial E}{\partial v_{t,n}} = -K\Big[\left(1 - \frac{b+1}{f}\right)(-z_{t,n} + v_{t,n}) + \left(1 - \frac{b+1}{f}\cos^2(\beta)\right)(-z_{t-1,n+1} + v_{t,n}) \\
&- \frac{b+1}{2f}\sin(2\beta)(-w_{t-1,n+1} + u_{t,n}) \\
&+ \left(1 + \frac{b-1}{s}\sin^2\left(\frac{\beta}{2}\right)\right)(3v_{t,n} - v_{t,n+1} - v_{t,n-1} - z_{t,n-1}) + \left(1 + \frac{b-1}{s}\sin^2\left(\frac{3\beta}{2}\right)\right)(-z_{t-1,n} + v_{t,n}) \\
&+ \frac{b-1}{2s}\sin(\beta)(u_{t,n+1} + u_{t,n-1} - u_{t,n} - w_{t,n-1}) + \frac{b-1}{2s}\sin(3\beta)(-u_{t,n} + w_{t-1,n})\Big] \\
M\ddot{z}_{t,n} &= -\frac{\partial E}{\partial z_{t,n}} = -K\Big[\left(1 - \frac{b+1}{f}\right)(-v_{t,n} + z_{t,n}) + \left(1 - \frac{b+1}{f}\cos^2(\beta)\right)(z_{t,n} - v_{t+1,n-1}) \\
&- \frac{b+1}{2f}\sin(2\beta)(w_{t,n} - u_{t+1,n-1}) \\
&+ \left(1 + \frac{b-1}{s}\sin^2\left(\frac{\beta}{2}\right)\right)(3z_{t,n} - v_{t,n+1} - z_{t,n+1} - z_{t,n-1}) + \left(1 + \frac{b-1}{s}\sin^2\left(\frac{3\beta}{2}\right)\right)(z_{t,n} - v_{t+1,n}) \\
&+ \frac{b-1}{2s}\sin(\beta)(-u_{t,n+1} - w_{t,n} + w_{t,n+1} + w_{t,n-1}) + \frac{b-1}{2s}\sin(3\beta)(u_{t+1,n} - w_{t,n})\Big]
\end{aligned}
\tag{S23}
$$

We now assume a solution of the form

$$
\begin{aligned}
u_{t,n} &= Ue^{i(k_t t + k_n n - \omega_{\vec{k}} t)} \\
w_{t,n} &= We^{i(k_t t + k_n n - \omega_{\vec{k}} t)} \\
v_{t,n} &= Ve^{i(k_t t + k_n n - \omega_{\vec{k}} t)} \\
z_{t,n} &= Ze^{i(k_t t + k_n n - \omega_{\vec{k}} t)}
\end{aligned}
\tag{S24}
$$

and obtain the following linear equation

$$
\begin{pmatrix}
A - \frac{M\omega^2}{K} & E & C & F \\
E & B - \frac{M\omega^2}{K} & F & D \\
C^* & F^* & A - \frac{M\omega^2}{K} & E \\
F^* & D^* & E & B - \frac{M\omega^2}{K}
\end{pmatrix}
\begin{pmatrix} U \\ V \\ W \\ Z \end{pmatrix} = 0
\tag{S25}
$$

with

$$
\begin{aligned}
A &\equiv 3-\frac{b+1}{f}\sin^2(\beta)+\left(1+\frac{b-1}{s}\cos^2\left(\frac{\beta}{2}\right)\right)(3-2\cos(k_n))+\frac{b-1}{s}\cos^2\left(\frac{3\beta}{2}\right)\\
B &\equiv 3-\frac{b+1}{f}\left(1+\cos^2(\beta)\right)+\left(1+\frac{b-1}{s}\sin^2\left(\frac{\beta}{2}\right)\right)(3-2\cos(k_n))+\frac{b-1}{s}\sin^2\left(\frac{3\beta}{2}\right)\\
C &\equiv -1+\left(\frac{b+1}{f}\sin^2(\beta)-1\right)e^{i(k_n-k_t)}-\left(1+\frac{b-1}{s}\cos^2\left(\frac{\beta}{2}\right)\right)e^{-ik_n}-\left(1+\frac{b-1}{s}\cos^2\left(\frac{3\beta}{2}\right)\right)e^{-ik_t}\\
D &\equiv \frac{b+1}{f}-1+\left(\frac{b+1}{f}\cos^2(\beta)-1\right)e^{i(k_n-k_t)}-\left(1+\frac{b-1}{s}\sin^2\left(\frac{\beta}{2}\right)\right)e^{-ik_n}-\left(1+\frac{b-1}{s}\sin^2\left(\frac{3\beta}{2}\right)\right)e^{-ik_t}\\
E &\equiv -\frac{b+1}{2f}\sin(2\beta)+\frac{b-1}{2s}\sin(\beta)\left(2\cos(k_n)-1\right)-\frac{b-1}{2s}\sin(3\beta)\\
F &\equiv \frac{b+1}{2f}\sin(2\beta)e^{i(k_n-k_t)}-\frac{b-1}{2s}\sin(\beta)e^{-ik_n}+\frac{b-1}{2s}\sin(3\beta)e^{-ik_t}
\end{aligned}
\tag{S26}
$$

where we have suppressed the index $\vec{k}$ from ω, A, B, C, D, E, and F.

Note that the logical indices for the position of each particle on the network are in the range $1 \le m,n \le L$, therefore $1 \le t \le L/2$, and $k_t = 4\pi p/L$ with $1 \le p \le L/2$ while $k_n = 2\pi q/L$ with $1 \le q \le L$. It is easy to see that these wavevectors are all compatible with the periodic boundary conditions, that all modes are different, and that the number of modes is equal to the number of degrees of freedom. Therefore this is a legitimate choice of representation for the normal modes, which is clearly much simpler than using real-space plane waves, which would yield a complicated Brillouin zone for such zigzagging stripes.

Requiring that the determinant of (S25) vanishes yields a quartic equation in ω^2 with solutions corresponding to the four branches $\omega_1^2(\vec{k}),\omega_2^2(\vec{k}),\omega_3^2(\vec{k}),\omega_4^2(\vec{k})$ of the dispersion relation. Again, to calculate $\mathcal{A} \equiv \frac{1}{N}\sum_k \log\left(\sqrt{\frac{M}{K}}\omega_k^2\right)$ we only need the product of the eigenfrequencies. It is straightforward to see that the product of the roots of the determinant in (S25) is given by

$$
\begin{aligned}
\left(\frac{M}{K}\right)^4\omega_1^2(\vec{k})\omega_2^2(\vec{k})\omega_3^2(\vec{k})\omega_4^2(\vec{k}) &= A^2B^2-B^2|C|^2+|C|^2|D|^2-A^2|D|^2+(E^2-|F|^2)^2\\
&- 2AB(E^2+|F|^2)+2E\left[A(D^*F+DF^*)+B(C^*F+CF^*)\right]\\
&- E^2(C^*D+CD^*)-(C^*D^*F^2+CD(F^*)^2)
\end{aligned}
\tag{S27}
$$

Technically, instead of taking the continuum limit and calculating $\mathcal{A}=\int d\vec{k}\log(\omega^2(\vec{k}))$, we calculate the discrete sum over modes in a finite system and verify numerically that the system is large enough. Care should be taken when dealing with the two zero-frequency modes of the system;, since including them in the sum would cause it to diverge. However, they are identical for straight stripes and for zigzagging stripes, therefore we ignore them in both cases. In contrast to the straight stripe situation, here there are four modes at $\vec{k}=0$, two of which have $\omega=0$ and two with $\omega>0$. It is easy to see that the product of these two non-zero frequencies is given by

$$
\left(\frac{M}{K}\right)^2\omega_1^2(0)\omega_2^2(0)=4(AB-E^2). \tag{S28}
$$

To write the dispersion relations in terms of (q_x,q_y) we note that the position of the unit cells (t,n) is given by $x=x_2m+\frac{af}{2}n$, $y=ahn+y_2m$. By requiring $q_xx+q_yy=k_tt+k_nn$, we obtain $k_t=q_xx_2+q_yy2$, $k_n=\frac{f}{2}q_x+ah$. As for the straight stripes, this may be used to verify that the logical approach described here and the physical approach described below both give the exact same dispersion relations.

C. Comparing Straight and Bent Stripes

To compare the dispersion relations and the resulting free energy of straight vs bent stripes, we first write the straight stripe results using a two-particle unit cell. In this way instead of having two branches in a $2\pi X2\pi$ region in (k_m,k_n) space, we will have four branches in a $\pi X2\pi$ region, as for the bent stripes. The two additional branches are simply the two single-particle-unit-cell branches from $k_m+\pi$. Figures S3,S4,S5,S6,S7,S8,S9 show the dispersion relations for straight and for bent stripes.

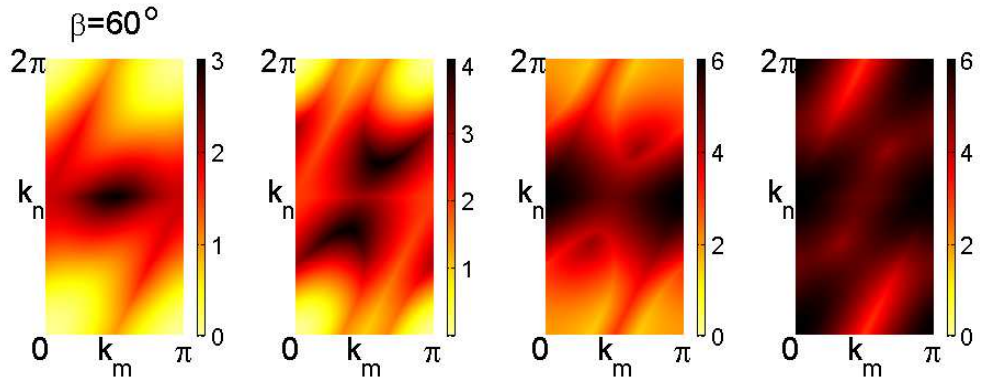

FIG. S3: Dispersion relations for the undeformed lattice.

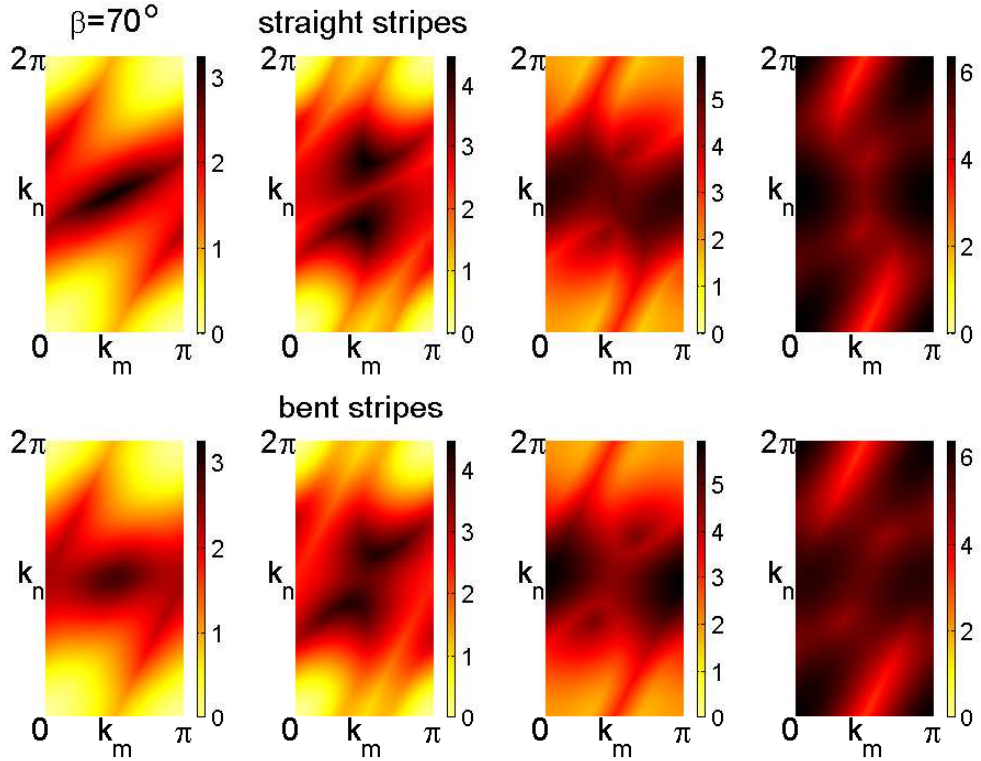

FIG. S4: Dispersion relations for a deformation of $\beta = 70°$.

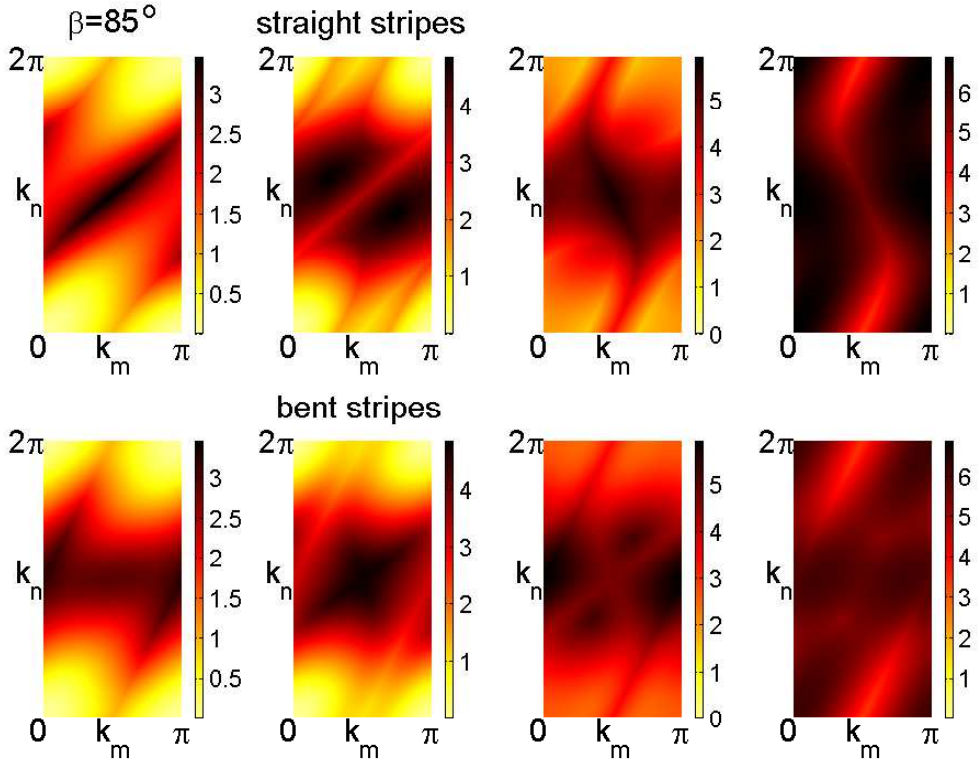

FIG. S5: Dispersion relations for a deformation of $\beta = 85°$.

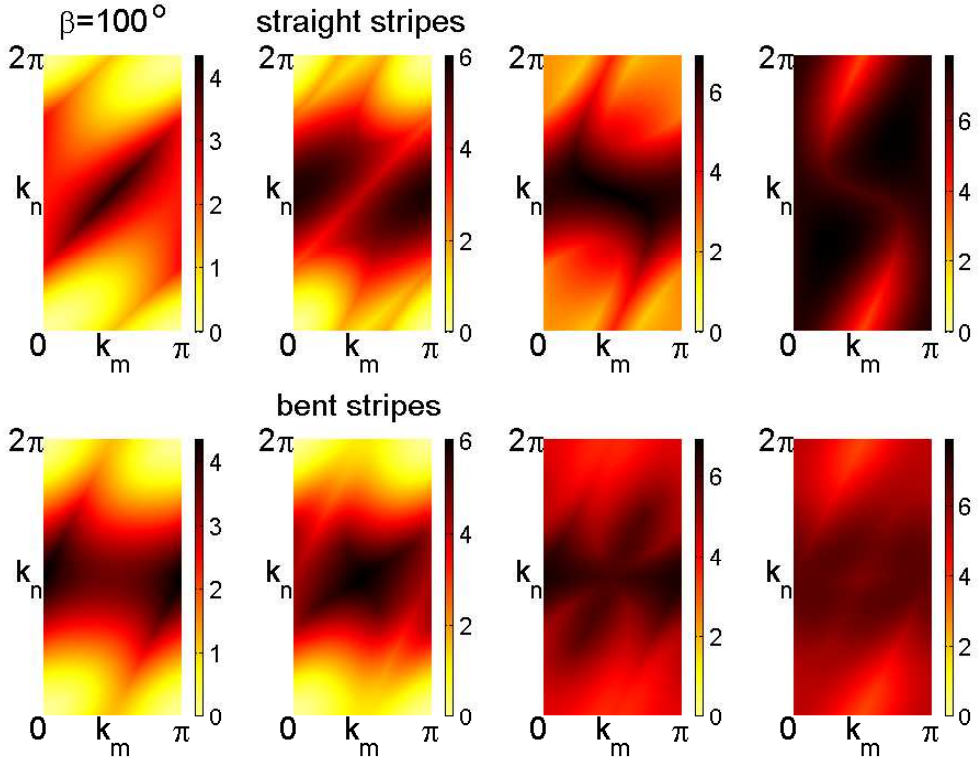

FIG. S6: Dispersion relations for a deformation of $\beta = 100°$.

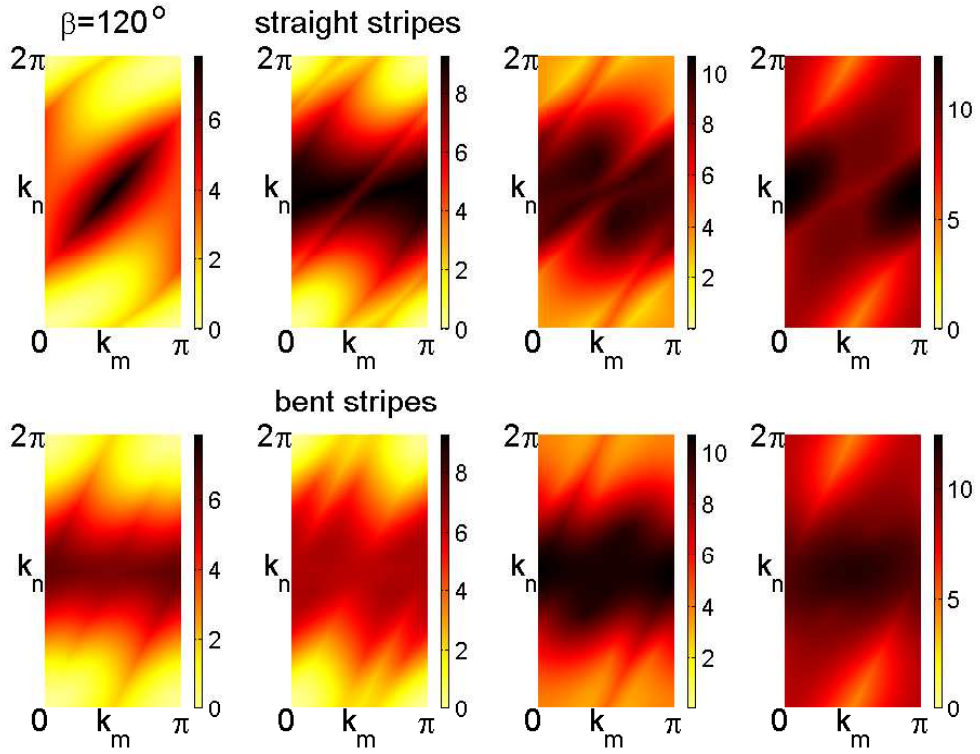

FIG. S7: Dispersion relations for a deformation of $\beta = 120°$.

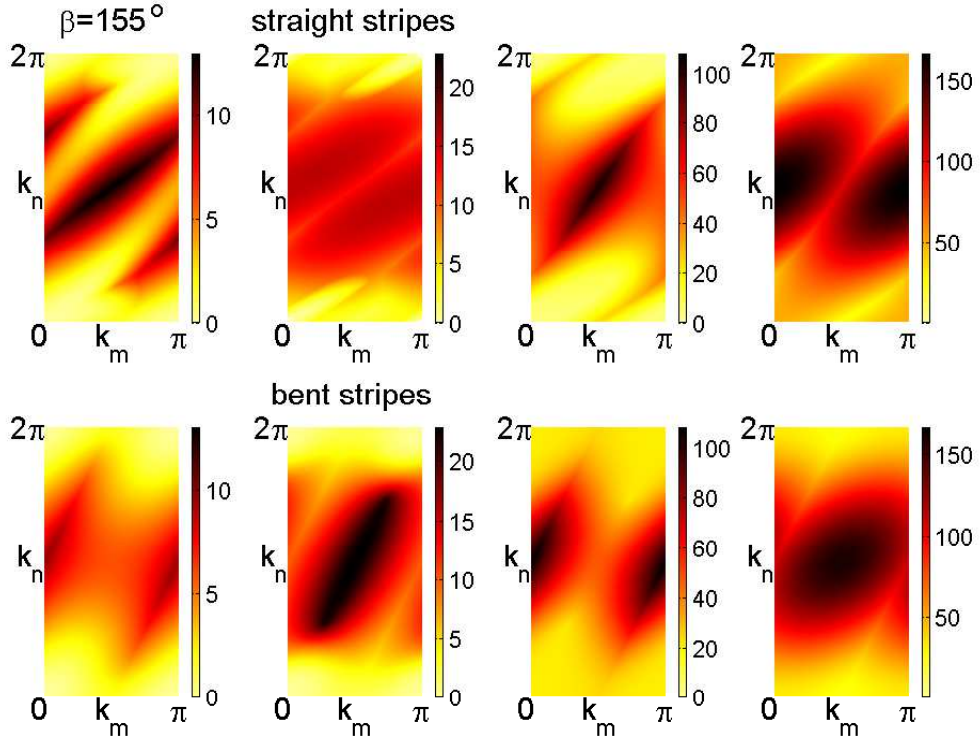

FIG. S8: Dispersion relations for a deformation of $\beta = 155°$.

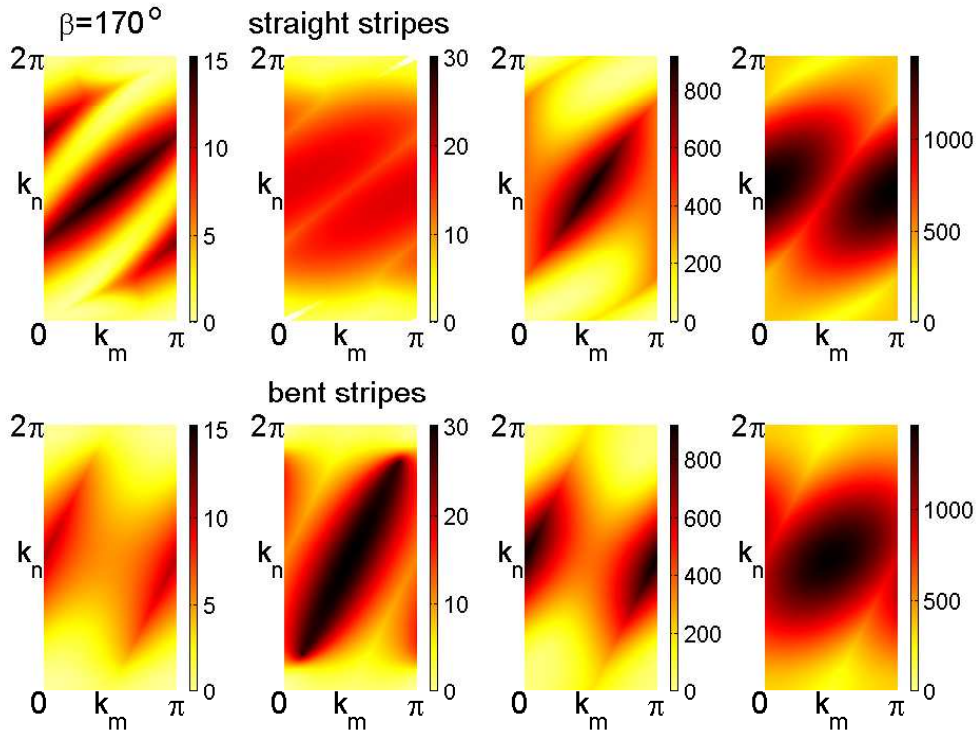

FIG. S9: Dispersion relations for a deformation of $\beta = 170°$.

The free-energy coefficient $\mathcal{A}$ is determined by the integral over $\vec{k}$ of the logarithm of the product of the four branches of the dispersion relations. In Fig. S10 we show the difference in the logarithm of the product of the four branches of the dispersion relations between straight and bent stripes. The integral of this quantity over $\vec{k}$ gives the free-energy difference $\mathcal{A}_0 - \mathcal{A}_1$ plotted in Fig 6D as a function of the deformation angle β. We see that the maximal difference grows monotonically with β (see the increasing color scale in the different panels), however the width of the region contributing positively to the free energy difference decreases as β increases. The combination of these two monotonic behaviors gives rise to the non-monotonic behavior of $\mathcal{A}_0 - \mathcal{A}_1$ seen in Fig 6D in the paper. Moreover, from the form at $\beta = 170°$ we see that at such extremely large deformation something qualitatively different happens and this is what eventually leads to the second increase in $\mathcal{A}_0 - \mathcal{A}_1$ at large β. Finally, to emphasize how small the difference in free energy between straight stripes and bent stripes is, we show in Fig. S11 the free energy coefficients $\mathcal{A}_0$ and $\mathcal{A}_1$.

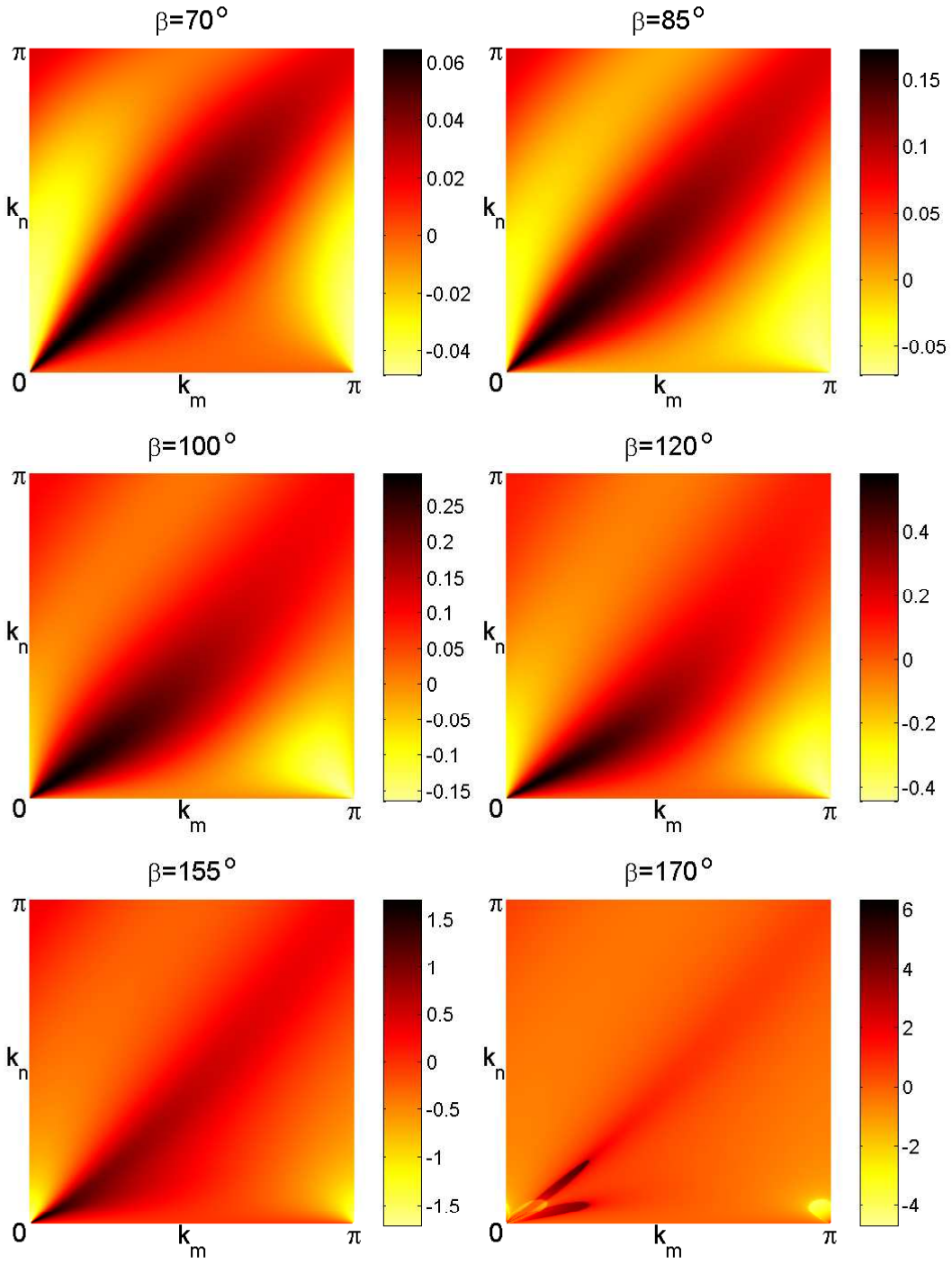

FIG. S10: The difference in the logarithm of the product of the four branches of the dispersion relations between straight and bent stripes.

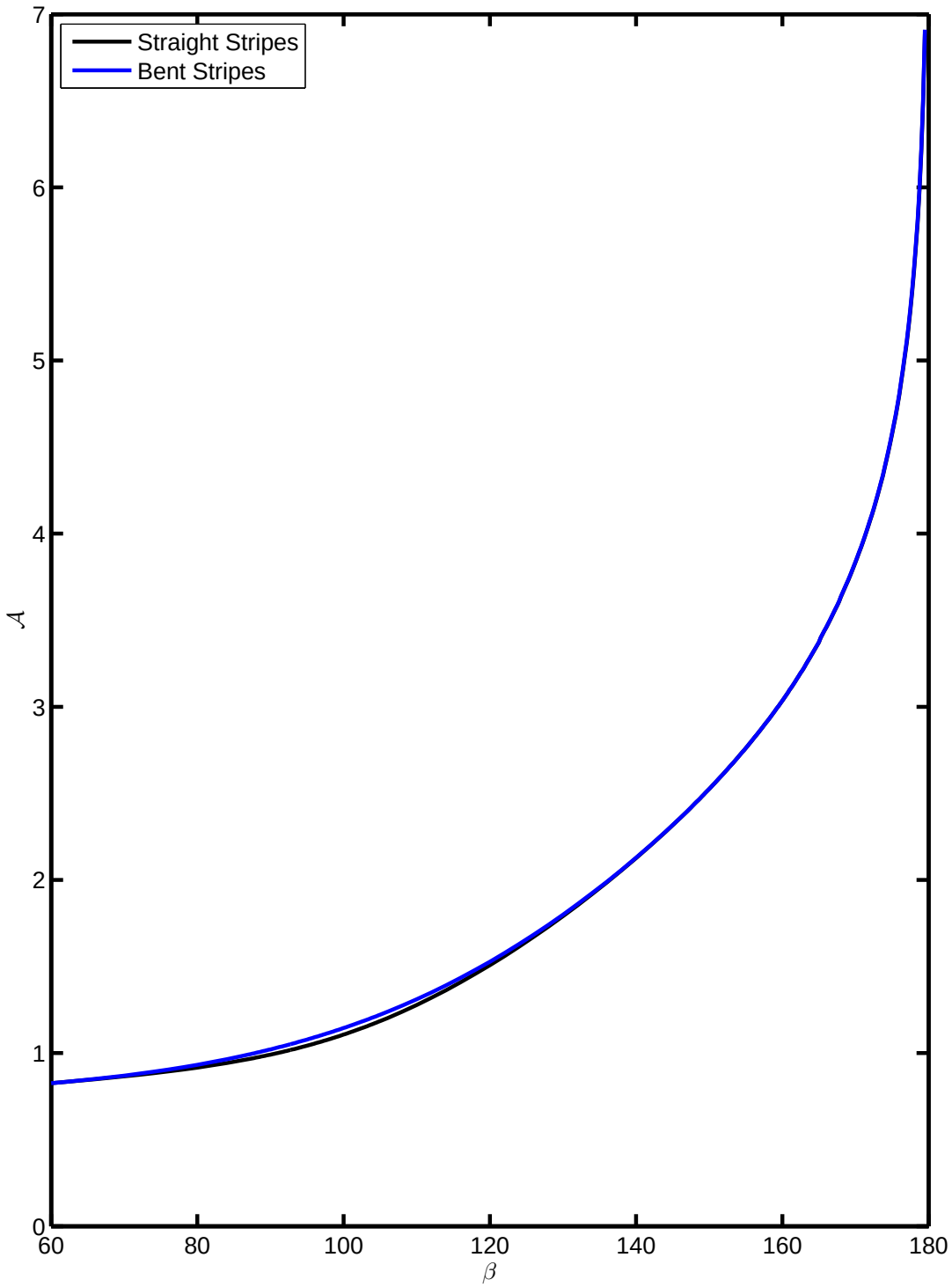

FIG. S11: Free energy coefficient for straight and bent stripes.

III. DISPERSION RELATIONS IN TERMS OF PHYSICAL WAVEVECTORS

The conventional approach to calculating the phonon spectra involves taking the Fourier transform of the space variables in the Hamiltonian, resulting in a quadratic form called the dynamical matrix. We note that in a particular ground state configuration the spins will relax to satisfy the minimum energy configuration of each triangle, as above. Thus, we can look at small displacements around those states, integrate out the phonon modes and find the contribution to the free energy for each configuration. More precisely, the partition function for a particular spin configuration is

$$Z = \int [D\mathbf{u}(\mathbf{q})] e^{-\frac{\beta}{2}\int \mathbf{u}^\dagger(\mathbf{q}) D(\mathbf{q}) \mathbf{u}(\mathbf{q}) d\mathbf{q}} \tag{S29}$$

where $D(\mathbf{q})$ is the dynamical matrix. Performing the integral, we get the free energy,

$$\mathcal{F} = -k_B T \ln Z = -k_B T V \ln \sqrt{k_B T \frac{(2\pi)^{dn}}{\det D}} = \frac{k_B T V}{2} \int \frac{d\mathbf{q}}{4\pi^2} \ln \det D(\mathbf{q}) + \text{const.} \tag{S30}$$

where $d = 2$ is the dimensionality of the system, n is the number of particles per unit cell chosen and V is the area of the lattice. Thus, the main effort is to calculate the determinant of the dynamical matrix, and the resulting integral.

Again we calculate the phonon entropies for the two configurations, straight and bent stripes, by linearizing the Hamiltonian about the ground state and performing the Fourier transform. Afterwards, we use the dynamical matrix to calculate the above integral over the first Brillouin zone of the lattices. The results obtained from taking this q-space approach agree with the k-space results presented above, as expected.

A. Linearized Hamiltonian

The Hamiltonian in Eq. (1) of the paper can be expressed in terms of the dispacements of the particles from their equilibrium positions, $\mathbf{u} = \mathbf{r} - \mathbf{r}_o$. For a fixed ground state spin configuration, this is simply a lattice of particles and springs, with a particular quadratic displacement energy associated with each bond. Since we expect mechanical stability, there can be no linear term in the displacement. Thus, we can write the contribution of each frustrated/satisfied bond as

$$\frac{K}{2} D_{kl}^{f/s}(\hat{e}^{ij}) \delta\mathbf{u}_k \delta\mathbf{u}_l \tag{S31}$$

where $\delta\mathbf{u} = \mathbf{u}^i - \mathbf{u}^j$ for a bond between particles i and j, pointing along the unit vector $\hat{e}^{ij}$.

Here,

$$D_{kl}^{f}(\hat{e}^{ij}) = \hat{e}_k^{ij}\hat{e}_l^{ij} + \frac{-b+f-1}{f}(\mathbb{I}_{kl} - \hat{e}_k^{ij}\hat{e}_l^{ij}) \tag{S32}$$

and

$$D_{kl}^{s}(\hat{e}^{ij}) = \hat{e}_k^{ij}\hat{e}_l^{ij} + \frac{b+s-1}{s}(\mathbb{I}_{kl} - \hat{e}_k^{ij}\hat{e}_l^{ij}) \tag{S33}$$

Note that the term proportional to $b = \epsilon J/Ka$ comes from expanding the spin-dependent term in the Hamiltonian $\epsilon\sigma_i\sigma_j |\mathbf{r}_i - \mathbf{r}_j|$, thus resulting in different signs. It effectively changes the relaxed length of the spring. The rest of the terms arise from expanding $\frac{1}{2}k_{ij}\left(|\mathbf{r}_i - \mathbf{r}_j| - a_{ij}\right)^2$ and correspond to the energy of stressed springs at equilibrium.

B. Straight Stripes

Straight stripes form a true Bravais lattice, with centered rectangular symmetry. It is possible to write down their Hamiltonian to linear order in terms of the neighbor interactions,

$$\mathcal{H} = \frac{K}{2}\sum_i \left(D_{kl}^{f}(\hat{x})\delta\mathbf{u}_k^{\hat{x}}\delta\mathbf{u}_l^{\hat{x}} + D_{kl}^{s}(\hat{e}_\alpha)\delta\mathbf{u}_k^{\hat{e}_\alpha}\delta\mathbf{u}_l^{\hat{e}_\alpha} + D_{kl}^{s}(\hat{e}_{-\alpha})\delta\mathbf{u}_k^{\hat{e}_\alpha}\delta\mathbf{u}_l^{\hat{e}_\alpha} \right) \tag{S34}$$

Since the ground state depends on the parameter $\alpha = \frac{1}{2}(\pi - \beta)$, the smaller angle of the isosceles triangle, so does the dynamical matrix, with $\hat{e}_{\pm\alpha} = (\cos\alpha, \pm\sin\alpha)$.

For a Bravais lattice, due to the inversion symmetry for all bonds, the dynamical matrix has a simple form. Using $\delta s = b + s - 1$ and $\delta f = -b + f - 1$, we define

$$M_{\pm} = \begin{bmatrix} \cos^2\alpha - \frac{\delta s}{s}\sin^2\alpha & \pm\left(1+\frac{\delta s}{s}\right)\sin\alpha\cos\alpha \\ \pm\left(1+\frac{\delta s}{s}\right)\sin\alpha\cos\alpha & \sin^2\alpha - \frac{\delta s}{s}\cos^2\alpha \end{bmatrix} \tag{S35}$$

and write the dynamical matrix as

$$D(\mathbf{q}) = 4K\left(\sin^2\left(\frac{f}{2}q_x\right)\begin{bmatrix} 1 & 0 \\ 0 & \frac{\delta f}{f} \end{bmatrix} + \sin^2\left(\frac{s}{2}\mathbf{q}\cdot\hat{e}_{\alpha}\right)M_{+} + \sin^2\left(\frac{s}{2}\mathbf{q}\cdot\hat{e}_{-\alpha}\right)M_{-}\right) \tag{S36}$$

The modes that make up the phonon spectrum can be plotted for several values of the angle β, as seen in Figs. S12, S13, S14, S15.

Finding the determinant seems challenging, while the integral – analytically unapproachable. However, this expression can be calculated numerically, justifying this approach.

The challenge would be then to find the Brillouin zone of the lattice, to properly perform the integral. This needs to be spit up into two problems, one for $\alpha > \pi/4$ and one for $\alpha < \pi/4$. In the marginal case $\alpha = \pi/4$, the Brillouin zone becomes square, while the orientation of the hexagon changes.

For $\alpha > \pi/4$ the orientation mimics that of the triangular lattice. We then define the Brillouin zone by vertices at the x-intercept and the one away from the axes. The shape retains its mirror symmetries across both of the axes, so these two points' reflections produce a hexagon. The x-intercept is at

$$\mathbf{v}_1 = \left(\frac{\pi}{\sqrt[4]{3}}\frac{1}{\cos^{1/2}\alpha\sin^{3/2}\alpha}, 0\right), \tag{S37}$$

while the other point –

$$\mathbf{v}_2 = \frac{\pi}{\sqrt[4]{3}}\left(2\cot^{1/2}\alpha, -\frac{\cos 2\alpha}{\cos^{1/2}\alpha\sin^{3/2}\alpha}\right). \tag{S38}$$

For large deformations with $\alpha < \pi/4$ we get instead the y-intercept at

$$\mathbf{v}_1 = \left(0, \frac{\pi}{\sqrt[4]{3}}\frac{1}{\cos^{3/2}\alpha\sin^{1/2}\alpha}\right) \tag{S39}$$

and the point

$$\mathbf{v}_2 = \frac{\pi}{\sqrt[4]{3}}\left(2\tan^{1/2}\alpha, \frac{\cos 2\alpha}{\cos^{3/2}\alpha\sin^{1/2}\alpha}\right) \tag{S40}$$

to be the vertices.

Another way to approach the problem would be to use the rectangular symmetry of the lattice, where two particles need to be put into a unit cell. We define then $\delta\mathbf{u}^{\hat{e}}_{ij} = \mathbf{u}_i(\mathbf{x}) - \mathbf{u}_j(\mathbf{x} + L\hat{e})$, where the indices indicate the particle within the unit cell, while $\hat{e}$ the direction of translation to the neighboring cell.

In this basis, the Hamiltonians for the bent and straight stripes look very similar. For the straight stripes, we have

$$\mathcal{H} = \frac{K}{2}\sum_i [D^s_{kl}(\hat{e}_{\alpha})\delta\mathbf{u}^{\mathbf{0}}_{12k}\delta\mathbf{u}^{\mathbf{0}}_{12l} \tag{S41}$$

$$+ D^f_{kl}(\hat{x})\left(\delta\mathbf{u}^{\hat{x}}_{22k}\delta\mathbf{u}^{\hat{x}}_{22l} + \delta\mathbf{u}^{\hat{x}}_{11k}\delta\mathbf{u}^{\hat{x}}_{11l}\right) + D^s_{kl}(\hat{e}_{\alpha})\delta\mathbf{u}^{\hat{e}_{\alpha}}_{12k}\delta\mathbf{u}^{\hat{e}_{\alpha}}_{12l} \tag{S42}$$

$$+ D^s_{kl}(\hat{e}_{-\alpha})\left(\delta\mathbf{u}^{\hat{x}}_{12k}\delta\mathbf{u}^{\hat{x}}_{12l} + \delta\mathbf{u}^{\hat{y}}_{12k}\delta\mathbf{u}^{\hat{y}}_{12l}\right)] \tag{S43}$$

The dynamical matrix, and from that the determinant, can be found analytically, but the expressions are too complicated to be of any use. However, its logarithm can be integrated numerically. Since the translation vectors are $(f, 0)$ and $(0, 2s\sin\alpha)$, the Brillouin zone can also be delineated. It corresponds to a rectangle

$$q_x \in \left[-\frac{\pi}{\sqrt[4]{3}}\sqrt{\tan\alpha}, \frac{\pi}{\sqrt[4]{3}}\sqrt{\tan\alpha}\right] \tag{S44}$$

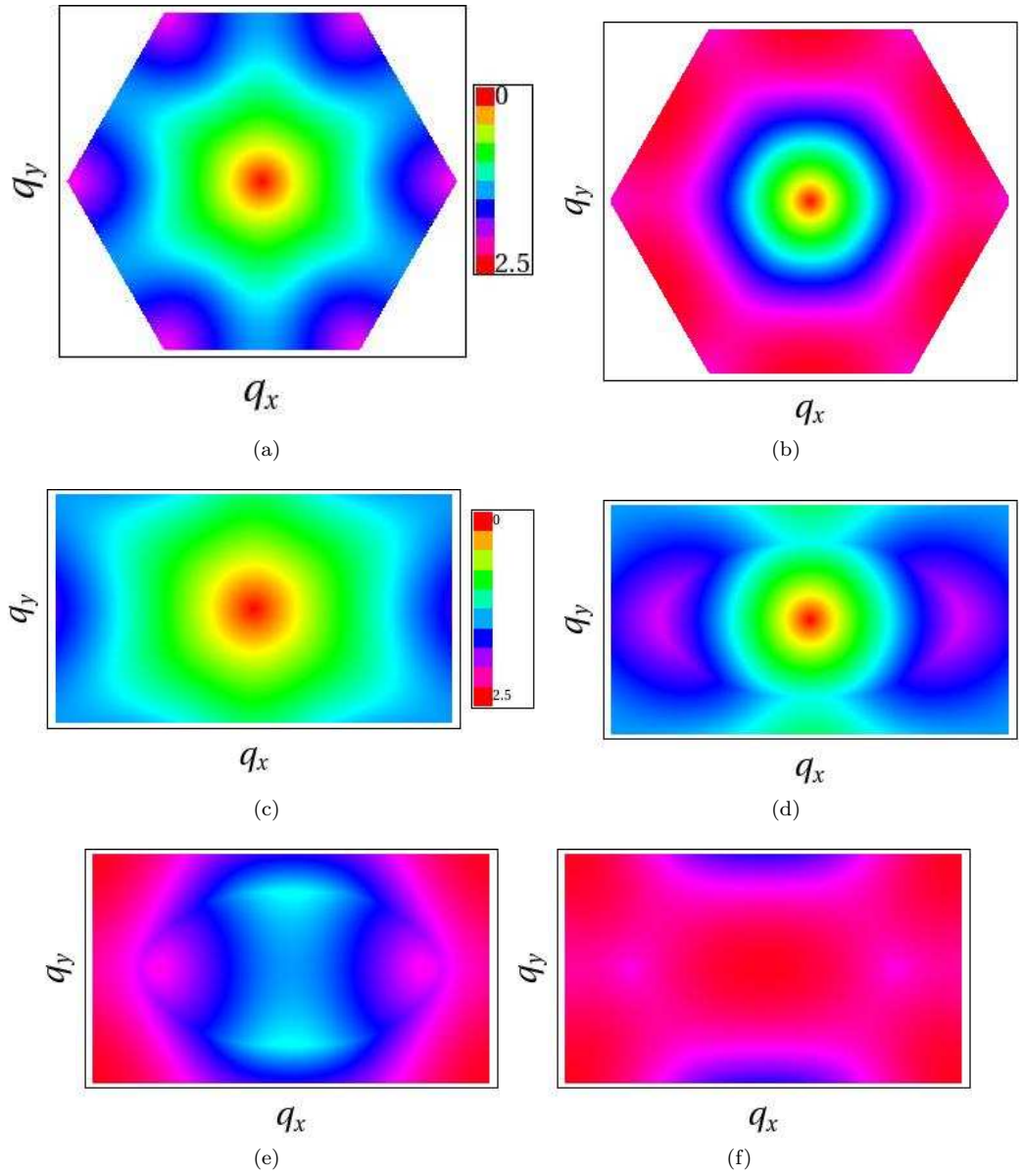

FIG. S12: The Brillouin zones and the different branches of the phonon dispersion spectra $\omega(\mathbf{q})$ for the triangular lattice, using both the primitive unit cell (a-b) and a rectangular unit cell (c-f) with two particles. This lattice corresponds to the $b = 0$ limit of our model, in which straight and bent stripes are indistinguishable.

and

$$q_y \in \left[-\frac{\pi}{\sqrt[4]{3}} \sqrt{\cot \alpha}, \frac{\pi}{\sqrt[4]{3}} \sqrt{\cot \alpha} \right]. \tag{S45}$$

We can plot the phonon spectrum, as seen in Figs. S12, S13, S14, S15. It is identitcal to the single particle basis spectrum, but is calculated using the two-particle basis within the rectangular Brillouin zone.

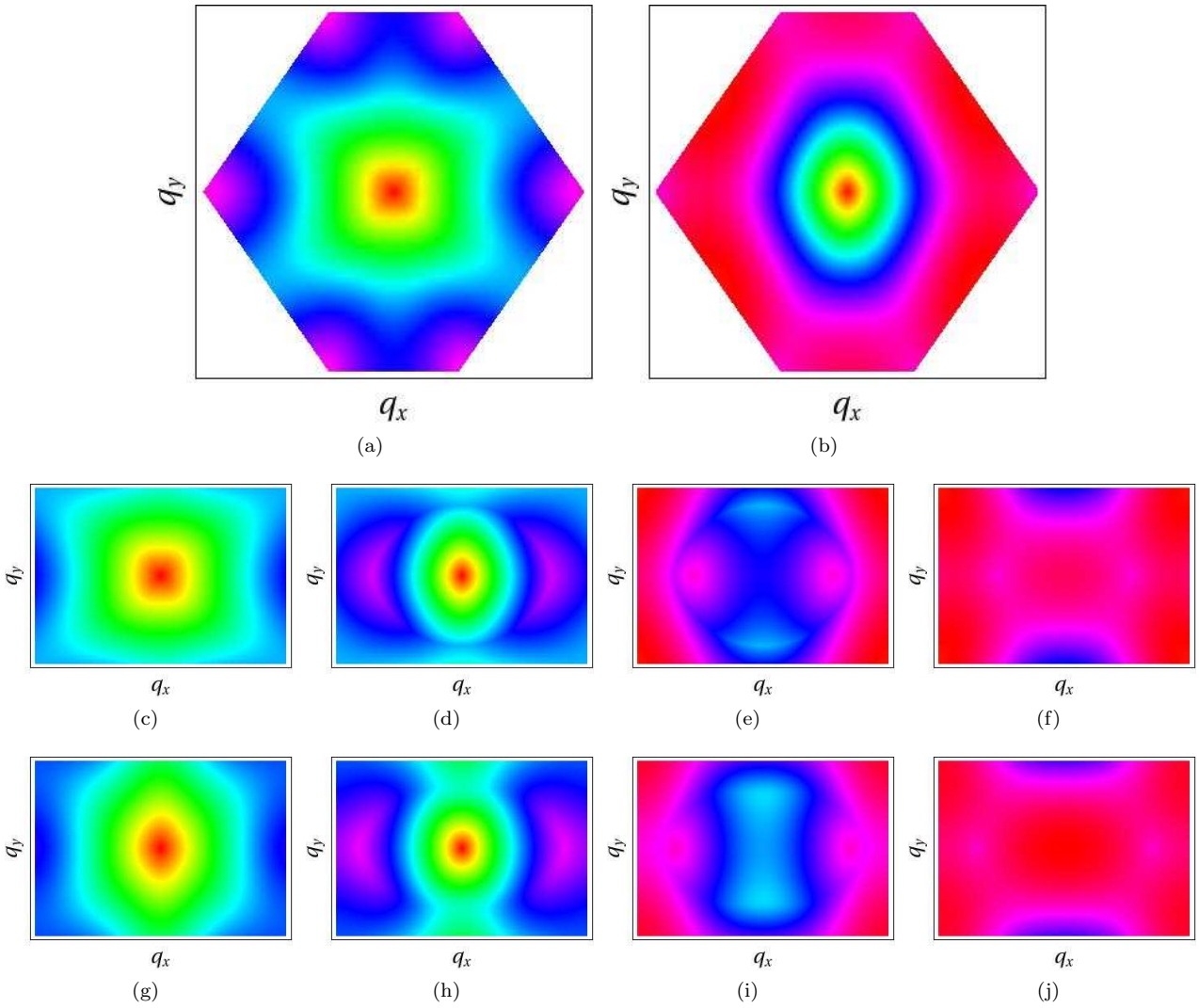

FIG. S13: The Brillouin zones and the phonon dispersion spectra $\omega(\mathbf{q})$ for lattices of straight (a-f) and bent (g-j) stripes with the deformation angle $\beta = 70°$. The scale is the same as in Fig. S12. (a) and (b) correspond to the two modes of the Bravais lattice basis for straight stripes, while (c-f) to the four modes in the two-particle rectangular lattice basis. For relatively small deformation angles, we see a small distortion of the BZ shape as well as a modification to the spectra. The spectra of bent and straight stripes as well as their BZ shapes are different.

C. Bent Stripes

Similarly, we get an expression for the bent stripes, though note that the neighbor distances are different in both directions,

$$\begin{aligned}
\mathcal{H} &= \frac{K}{2}\sum_i [D^f_{kl}(\hat{e}_\alpha)\delta\mathbf{u}^{\mathbf{0}}_{12k}\delta\mathbf{u}^{\mathbf{0}}_{12l} && \text{(S46)}\\
&+ D^s_{kl}(\hat{x})\left(\delta\mathbf{u}^{\hat{x}}_{22k}\delta\mathbf{u}^{\hat{x}}_{22l} + \delta\mathbf{u}^{\hat{x}}_{11k}\delta\mathbf{u}^{\hat{x}}_{11l}\right) && \text{(S47)}\\
&+ D^s_{kl}(\hat{e}_{2\alpha})\delta\mathbf{u}^{\hat{x}}_{12k}\delta\mathbf{u}^{\hat{x}}_{12l} + D^s_{kl}(\hat{e}_{-2\alpha})\delta\mathbf{u}^{\hat{t}}_{12k}\delta\mathbf{u}^{\hat{t}}_{12l} && \text{(S48)}\\
&+ D^f_{kl}(\hat{e}_{-\alpha})\left(\delta\mathbf{u}^{\hat{y}}_{12k}\delta\mathbf{u}^{\hat{y}}_{12l} + \delta\mathbf{u}^{\hat{y}}_{12k}\delta\mathbf{u}^{\hat{y}}_{12l}\right)] && \text{(S49)}
\end{aligned}$$

Here, the new notation is that of $\hat{t}$ is the unit vector along $(s, 2f\sin\alpha)$, translating in both lattice vectors.

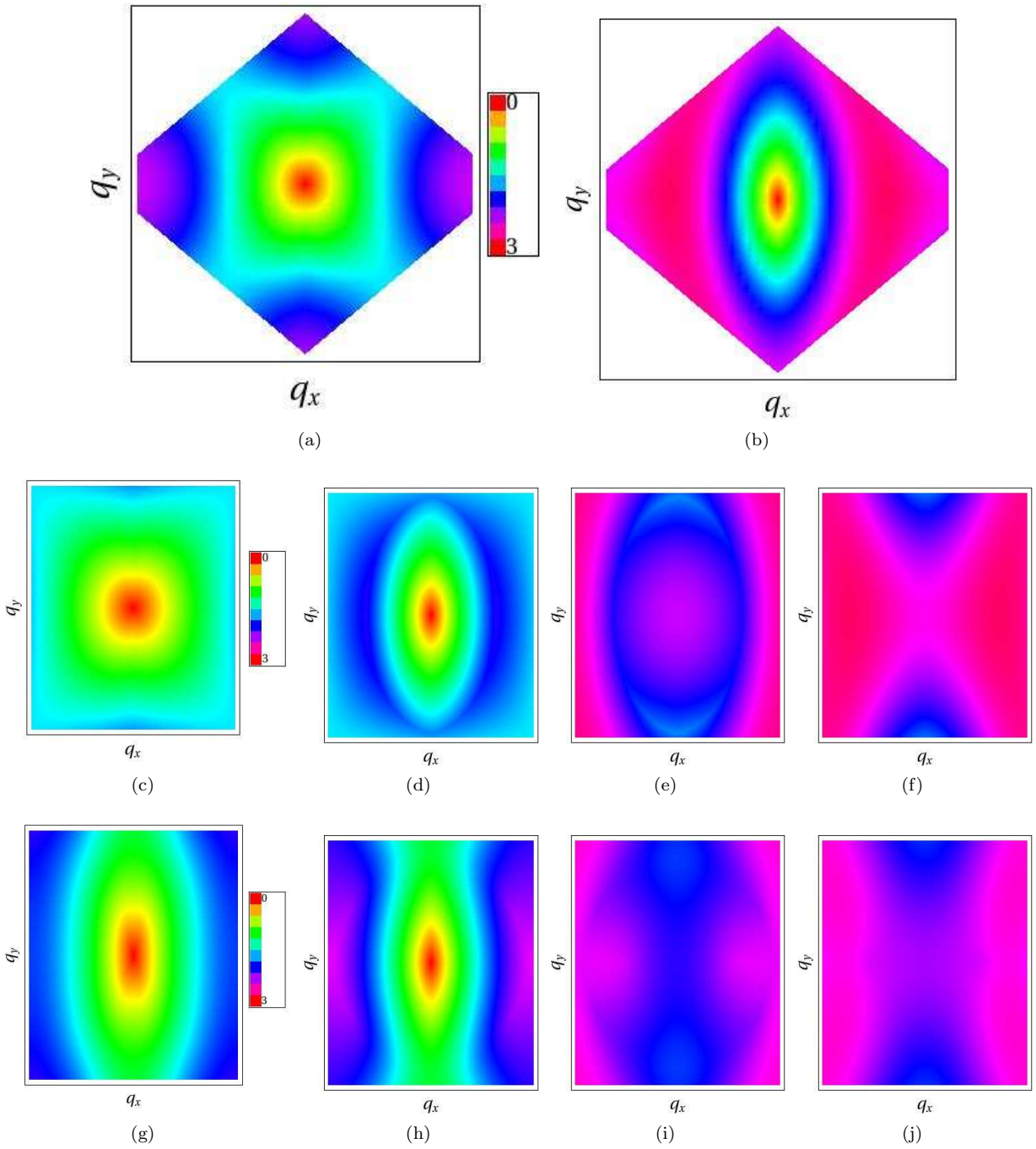

FIG. S14: The Brillouin zones and the phonon dispersion spectra $\omega(\mathbf{q})$ for lattices of straight (a-f) and bent (g-j) stripes with the deformation angle $\beta = 100°$. (a) and (b) correspond to the two modes of the Bravais lattice basis for straight stripes, while (c-f) to the four modes in the two-particle rectangular lattice basis. For larger deformation angles, we see dramatic changes in both the behavior of the spectrum as well as the shape of the BZ.

The lattice vectors are $\{s(1,0), 2f\sin\alpha(0,1)\}$. The Brillouin zone is then the region

$$q_x \in \left[-\frac{2\pi}{\sqrt[4]{3}}\sqrt{\cos\alpha\sin\alpha}, \frac{2\pi}{\sqrt[4]{3}}\sqrt{\cos\alpha\sin\alpha}\right] \tag{S50}$$

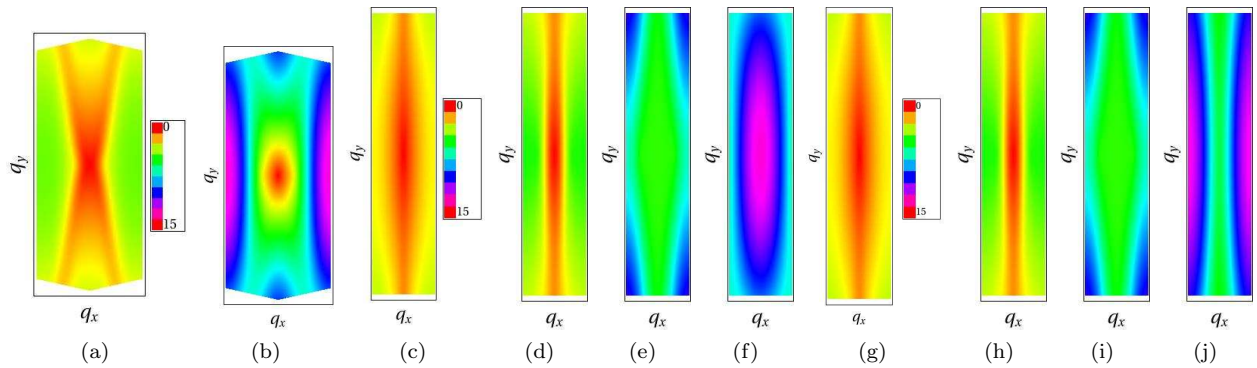

FIG. S15: The Brillouin zones and the phonon dispersion spectra $\omega(\mathbf{q})$ for lattices of straight (a-f) and bent (g-j) stripes with the deformation angle $\beta = 155°$. (a) and (b) correspond to the two modes of the Bravais lattice basis for straight stripes, while (c-f) to the four modes in the two-particle rectangular lattice basis. At extreme deformation angles, we see that the Brillouin zone extends significantly in one direction, while shrinking in the other. The phonon spectrum changes dramatically and can be easily observed to differ vastly in the two cases.

and

$$q_y \in \left[-\frac{\pi}{2\sqrt[4]{3}} \frac{1}{\sqrt{\cos\alpha \sin\alpha}}, \frac{\pi}{2\sqrt[4]{3}} \frac{1}{\sqrt{\cos\alpha \sin\alpha}} \right] \tag{S51}$$

The phonon spectrum for the bent stripes in different from that of the straight stripes. However, a direct comparison this way is more difficult than by in k-space described above, due to different shapes of the Brillouin zone.

D. Larger Unit Cells

The argument above concludes that the straight stripes have the highest phonon entropy, while the bent stripes have the lowest. However, this assumes that the other ground state configurations, have phonon entropy values intermediate between these two cases. It might be intuitive to think that the phonon entropy should have a strong dependence on the proportion of nearest neighbor configurations p_s. In order to show this, we calculate the phonon entropies for ordered ground state configurations with larger unit cells.

First, we construct the striped configurations. We know that one direction will always be periodic, corresponding to stripes of alternating spins. Defining the configuration allows us to place the spins in the other direction. Note that as in the previous examples, we only care about the types of bonds, rather than the values of the spins, thus halving the unit cell size. The configurations can be indexed as B_i, an ordered set of "0"s and "1"s of size S. A "1" ("0") at position i in the set indicates a frustrated bond between particles i and $i+1$ along the $\mathbf{f_1}$ ($\mathbf{f_2}$) direction. We take $\mathbf{f_1}$ to be along the x-axis, $\mathbf{f_1} = f(1,0)$. From our ground state calculations, we then know that $\mathbf{f_2} = f(-\cos 2\alpha, \sin 2\alpha)$. The last position in the array indicates the direction of the bond between the last particle in this unit cell and the first particle in the next unit cell.

Note that while each such array corresponds to a particular phonon entropy, these entropies will not be unique, since many of these arrays make essentially the same lattice. There are four redundancies –
(1) Switching all "0"s and "1"s corresponds to a rotation of the entire lattice.
(2) Making a cyclic permutation of the array corresponds to making a different choice of the unit cell.
(3) Arrays with periodic order (e.g. $\{0,1,1,0,1,1\}$)) correspond to a large unit cell choice for a lattice with a smaller unit cell (e.g. $\{0,1,1\}$). Thus, we index the lattices using the smallest possible choice of the unit cell.
(4) Reversing the order on the array corresponds to a parity transformation of the plane.

Once these redundancies are taken into account, we obtain a set of distinct lattices of zigzagging stripes, with some of the smaller unit cells detailed in Fig. 5. The index notation is indicated for these in the tables below. We can see that the number of configurations will necessarily scale as $O(2^S)$.

We take the first particle of the unit cell to be at $\mathbf{r}_1 = (0,0)$. For the rest of the particles, $i > 1$,

$$\mathbf{r}_i = \sum_{n=1}^{i-1} \mathbf{f_1} B_{i-1} + \mathbf{f_2}(1 - B_{i-1}). \tag{S52}$$

The primitive vectors for the underlying Bravais lattice are then $\mathbf{r}_{S+1}$ and $s(-\cos\alpha, \sin\alpha)$. This completely defines our lattice model and lets us calculate the dynamical matrix for these larger unit cell.

Bonds between particles i and j within the unit cell (which are all frustrated) will correspond to entries at the diagonal 2x2 blocks of the dynamical matrix for particles i and j, $KD^f_{kl}(\hat{e}^{ij})$. For the off-diagonal blocks indexed by i, j and j, i the entries are $-KD^f_{kl}(\hat{e}^{ij})$. Due to the linear nature of the Hamiltonian, the contributions of different bonds will simply add together.

Similarly, for bonds outside the unit cell, the frustrated bonds will contribute $KD^f_{kl}(\hat{e}^{ij})$ on the diagonal and $-\exp(\pm i\mathbf{q}\cdot\mathbf{l})KD^f_{kl}(\hat{e}^{ij})$ off the diagonal, where $\mathbf{l}$ is the corresponding vector of the Bravais lattice. The satisfied bonds have entries $KD^s_{kl}(\hat{e}^{ij})$ and $-\exp(\pm i\mathbf{q}\cdot\mathbf{l})KD^s_{kl}(\hat{e}^{ij})$. By summing all of these contributions, we obtain the dynamical matrix of this lattice, analogously to the derivations for the smaller unit cells.

This approach is in fact identical to taking the Fourier transform of Eq. (S41). As pointed out, the expressions for the dynamical matrix are quite cumbersome, though straight-forward since they can be broken up into these blocks. For a specific angle, the dynamical matrix can be determined numerically, making this approach much more useful.

Again, integrating the logarithm of the determinant of the dynamical matrix over the first Brillouin zone will give us the phonon entropies. However, the shape of the first Brillouin zones themselves may be difficult to determine. Instead, we can use the basis vectors for the Bravais lattice to construct a unit cell of the reciprocal lattice, and for simplicity map it into a rectangular region using a linear transformation of unity determinant. Thus, we can calculate $(\mathcal{A} - \mathcal{A}_1)/(\mathcal{A}_o - \mathcal{A}_1)$ for some range of the unit cell size S. For larger unit cells, the numerical integration over the unit cell becomes more computationally intensive and less precise. We were able to calculate this quantity for $S \leq 10$ for $\beta = 70°, 100°, 155°$ and for $11 \leq S \leq 13$ for $\beta = 70°, 100°$.

			$(\mathcal{A}-\mathcal{A}_1)/(\mathcal{A}_o-\mathcal{A}_1)$		
Configuration	S	p_s	$\beta = 70°$	$\beta = 100°$	$\beta = 155°$
{1}	1	1	1	1	1
{0,1}	2	0	0	0	0
* {0,1,1}	3	1/3	0.7339	0.7298	0.8318
* {0,1,1,1}	4	1/2	0.5601	0.5584	0.6822
* {0,1,1,0}	4	1/2	0.6209	0.6145	0.7850
{0,1,1,0,1}	5	1/5	0.8433	0.8399	0.9065
{0,1,1,1,1}	5	3/5	0.4508	0.4498	0.5794
{0,1,1,1,0}	5	3/5	0.5115	0.5067	0.6916
* {0,1,1,1,0,1}	6	1/3	0.7108	0.7088	0.7944
* {0,1,1,0,1,0}	6	1/3	0.7436	0.7397	0.8505
{0,1,1,1,1,1}	6	2/3	0.3767	0.3760	0.4953
{0,1,1,1,1,0}	6	2/3	0.4301	0.4273	0.6075
{0,1,1,1,0,0}	6	2/3	0.4399	0.4376	0.6355
{0,1,1,0,1,0,1}	7	1/7	0.8882	0.8859	0.9252
{0,1,1,1,1,0,1}	7	3/7	0.6112	0.6107	0.7103
{0,1,1,1,0,1,1}	7	3/7	0.6355	0.6321	0.7477
{0,1,1,1,0,0,1}	7	3/7	0.6476	0.6439	0.7757
{0,1,1,0,1,1,0}	7	3/7	0.6719	0.6650	0.8037
{0,1,1,1,1,1,1}	7	5/7	0.3232	0.3228	0.4299
{0,1,1,1,1,1,0}	7	5/7	0.3706	0.3685	0.5421
{0,1,1,1,1,0,0}	7	5/7	0.3827	0.3807	0.5794
{0,1,1,1,0,1,0,1}	8	1/4	0.7837	0.7821	0.8505
{0,1,1,0,1,1,0,1}	8	1/4	0.8019	0.7988	0.8785
{0,1,1,0,1,0,0,1}	8	1/4	0.8056	0.8017	0.8785
{0,1,1,0,1,0,1,0}	8	1/4	0.8080	0.8044	0.8879
*{0,1,1,1,1,1,0,1}	8	1/2	0.5358	0.5357	0.6355
*{0,1,1,1,1,0,1,1}	8	1/2	0.5577	0.5553	0.6729
*{0,1,1,1,1,0,0,1}	8	1/2	0.5699	0.5672	0.7009
*{0,1,1,1,0,1,0,0}	8	1/2	0.5747	0.5733	0.7196
*{0,1,1,1,0,1,1,0}	8	1/2	0.5942	0.5895	0.7477
*{0,1,1,1,0,0,1,0}	8	1/2	0.5966	0.5925	0.7477
{0,1,1,1,1,1,1,1}	8	3/4	0.2831	0.2827	0.3832
{0,1,1,1,1,1,1,0}	8	3/4	0.3244	0.3234	0.4766
{0,1,1,1,1,1,0,0}	8	3/4	0.3366	0.3356	0.5234
{0,1,1,1,1,0,0,0}	8	3/4	0.3390	0.3388	0.5327
{0,1,1,0,1,0,1,0,1}	9	1/9	0.9137	0.9112	0.9439
*{0,1,1,1,1,0,1,0,1}	9	1/3	0.6987	0.6979	0.7757
*{0,1,1,1,0,1,1,0,1}	9	1/3	0.7181	0.7155	0.8037
*{0,1,1,1,0,1,0,0,1}	9	1/3	0.7217	0.7195	0.8224
*{0,1,1,1,0,1,0,1,0}	9	1/3	0.7254	0.7228	0.8224
*{0,1,1,0,1,1,0,0,1}	9	1/3	0.7412	0.7369	0.8505
*{0,1,1,0,1,0,1,1,0}	9	1/3	0.7448	0.7402	0.8505
{0,1,1,1,1,1,1,0,1}	9	5/9	0.4775	0.4769	0.5701
{0,1,1,1,1,1,0,1,1}	9	5/9	0.4970	0.4947	0.6075
{0,1,1,1,1,0,1,1,1}	9	5/9	0.4994	0.4981	0.6262
{0,1,1,1,1,1,0,1,0}	9	5/9	0.5079	0.5059	0.6355
{0,1,1,1,1,0,1,0,0}	9	5/9	0.5152	0.5134	0.6636
{0,1,1,1,1,0,1,1,0}	9	5/9	0.5298	0.5268	0.6822
{0,1,1,1,0,1,1,1,0}	9	5/9	0.5334	0.5303	0.6916
{0,1,1,1,1,0,0,1,0}	9	5/9	0.5346	0.5308	0.6916
{0,1,1,1,0,1,1,0,0}	9	5/9	0.5371	0.5342	0.7009
{0,1,1,1,0,0,1,1,0}	9	5/9	0.5601	0.5549	0.7290
{0,1,1,1,1,1,1,1,1}	9	7/9	0.2515	0.2515	0.3364
{0,1,1,1,1,1,1,1,0}	9	7/9	0.2892	0.2880	0.4299
{0,1,1,1,1,1,1,0,0}	9	7/9	0.3001	0.2997	0.4766
{0,1,1,1,1,1,0,0,0}	9	7/9	0.3038	0.3038	0.4953

TABLE S4: Values plotted in Fig. 6(A-C) with the corresponding stripe configurations. The configurations shown in Fig. 5 are marked with a "*" and arranged in the same order as in Fig. 5.

			$(\mathcal{A}-\mathcal{A}_1)/(\mathcal{A}_o-\mathcal{A}_1)$		
Configuration	S	p_s	$\beta = 70^\circ$	$\beta = 100^\circ$	$\beta = 155^\circ$
{0,1,1,1,0,1,0,1,0,1}	10	1/5	0.8275	0.8259	0.8785
{0,1,1,0,1,1,0,1,0,1}	10	1/5	0.8420	0.8392	0.9065
{0,1,1,0,1,0,1,0,0,1}	10	1/5	0.8445	0.8411	0.9065
{0,1,1,0,1,0,1,0,1,0}	10	1/5	0.8469	0.8435	0.9065
{0,1,1,1,1,1,0,1,0,1}	10	2/5	0.6306	0.6293	0.7103
{0,1,1,1,1,0,1,1,0,1}	10	2/5	0.6488	0.6461	0.7477
{0,1,1,1,0,1,1,1,0,1}	10	2/5	0.6513	0.6487	0.7570
{0,1,1,1,1,0,1,0,0,1}	10	2/5	0.6525	0.6503	0.7477
{0,1,1,1,1,0,1,0,1,0}	10	2/5	0.6549	0.6534	0.7664
{0,1,1,1,0,1,0,0,0,1}	10	2/5	0.6561	0.6542	0.7757
{0,1,1,1,0,1,0,1,0,0}	10	2/5	0.6598	0.6581	0.7757
{0,1,1,1,0,1,1,0,1,1}	10	2/5	0.6659	0.6615	0.7757
{0,1,1,1,0,1,1,0,0,1}	10	2/5	0.6719	0.6687	0.7944
{0,1,1,1,0,1,1,0,1,0}	10	2/5	0.6731	0.6695	0.7944
{0,1,1,1,0,1,0,0,1,0}	10	2/5	0.6744	0.6707	0.7944
{0,1,1,1,0,1,0,1,1,0}	10	2/5	0.6768	0.6726	0.7944
{0,1,1,1,0,0,1,0,1,0}	10	2/5	0.6780	0.6745	0.8037
{0,1,1,0,1,1,0,1,1,0}	10	2/5	0.6902	0.6846	0.8131
{0,1,1,0,1,1,0,0,1,0}	10	2/5	0.6914	0.6857	0.8224
{0,1,1,0,1,0,0,1,1,0}	10	2/5	0.6950	0.6896	0.8224
{0,1,1,1,1,1,1,1,0,1}	10	3/5	0.4301	0.4295	0.5140
{0,1,1,1,1,1,1,0,1,1}	10	3/5	0.4471	0.4456	0.5514
{0,1,1,1,1,1,0,1,1,1}	10	3/5	0.4508	0.4490	0.5701
{0,1,1,1,1,1,1,0,1,0}	10	3/5	0.4569	0.4562	0.5794
{0,1,1,1,1,1,1,0,0,1}	10	3/5	0.4581	0.4562	0.5794
{0,1,1,1,1,1,0,1,0,0}	10	3/5	0.4642	0.4639	0.6168
{0,1,1,1,1,0,1,0,0,0}	10	3/5	0.4666	0.4659	0.6262
{0,1,1,1,1,1,0,1,1,0}	10	3/5	0.4787	0.4754	0.6262
{0,1,1,1,1,1,0,0,1,0}	10	3/5	0.4824	0.4798	0.6355
{0,1,1,1,1,0,1,1,1,0}	10	3/5	0.4824	0.4795	0.6355
{0,1,1,1,1,0,1,1,0,0}	10	3/5	0.4860	0.4838	0.6542
{0,1,1,1,1,0,0,1,0,0}	10	3/5	0.4872	0.4850	0.6542
{0,1,1,1,0,1,1,1,0,0}	10	3/5	0.4897	0.4871	0.6636
{0,1,1,1,1,0,0,1,1,0}	10	3/5	0.5067	0.5027	0.6822
{0,1,1,1,0,0,1,1,0,0}	10	3/5	0.5128	0.5078	0.6916
{0,1,1,1,1,1,1,1,1,1}	10	4/5	0.2260	0.2264	0.3084
{0,1,1,1,1,1,1,1,1,0}	10	4/5	0.2600	0.2595	0.3925
{0,1,1,1,1,1,1,1,0,0}	10	4/5	0.2710	0.2705	0.4393
{0,1,1,1,1,1,1,0,0,0}	10	4/5	0.2746	0.2750	0.4579
{0,1,1,1,1,1,0,0,0,0}	10	4/5	0.2758	0.2761	0.4673
{0,1,1,0,1,0,1,0,1,0,1}	11	1/11	0.9295	0.9276	–
{0,1,1,1,1,1,1,1,1,1,1}	11	9/11	0.2053	0.2059	–
{0,1,1,1,1,1,1,1,1,1,0}	11	9/11	0.2369	0.2361	–
{0,1,1,1,1,1,1,1,1,0,0}	11	9/11	0.2467	0.2463	–
{0,1,1,1,1,1,1,1,0,0,0}	11	9/11	0.2503	0.2508	–
{0,1,1,1,1,1,1,0,0,0,0}	11	9/11	0.2515	0.2525	–
{0,1,1,1,1,1,1,1,1,1,1,1}	12	5/6	0.1883	0.1887	–
{0,1,1,1,1,1,1,1,1,1,1,0}	12	5/6	0.2175	0.2165	–
{0,1,1,1,1,1,1,1,1,1,0,0}	12	5/6	0.2260	0.2262	–
{0,1,1,1,1,1,1,1,1,0,0,0}	12	5/6	0.2296	0.2304	–
{0,1,1,1,1,1,1,1,0,0,0,0}	12	5/6	0.2321	0.2325	–
{0,1,1,1,1,1,1,0,0,0,0,0}	12	5/6	0.2321	0.2330	–
{0,1,1,0,1,0,1,0,1,0,1,0,1}	13	1/13	0.9405	–	–
{0,1,1,1,1,1,1,1,1,1,1,1,1}	13	11/13	0.1738	0.1742	–
{0,1,1,1,1,1,1,1,1,1,1,1,0}	13	11/13	0.2005	0.1999	–
{0,1,1,1,1,1,1,1,1,1,1,0,0}	13	11/13	0.2090	0.2089	–
{0,1,1,1,1,1,1,1,1,1,0,0,0}	13	11/13	0.2126	0.2130	–
{0,1,1,1,1,1,1,1,1,0,0,0,0}	13	11/13	0.2139	0.2151	–
{0,1,1,1,1,1,1,1,0,0,0,0,0}	13	11/13	0.2151	0.2160	–

TABLE S5: Values plotted in Fig. 6(A-C) with the corresponding stripe configurations for larger unit cell sizes. For unit cells with 11 through 13 particles, only the values of $(\mathcal{A}-\mathcal{A}_1)/(\mathcal{A}_o-\mathcal{A}_1)$ which fall outside the range of the unit cells with 3 to 10 particles are shown.